Tribological Behavior of a Cr_2O_3 Ceramic Coating/Steel Couple Under Dry Sliding and Heavy Loading Conditions

C. Soffritti, M. Merlin, R. Vazquez & G. L. Garagnani

Journal of Materials Engineering and Performance

ISSN 1059-9495
Volume 27
Number 7

J. of Materi Eng and Perform (2018)
27:3699-3708
DOI 10.1007/s11665-018-3426-3

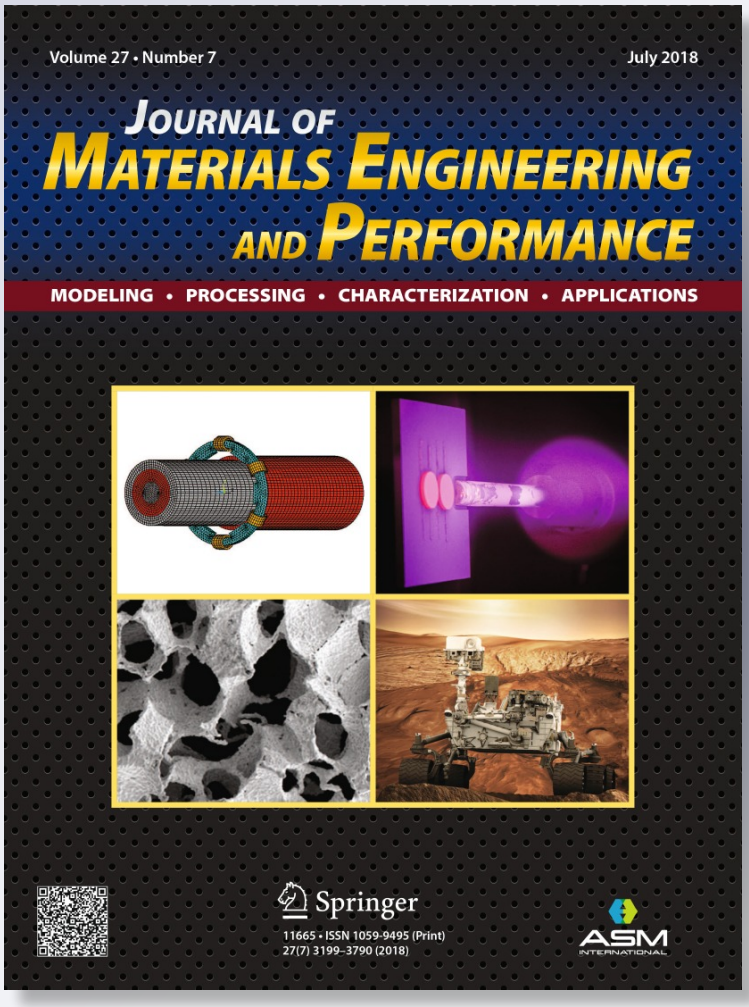

Springer

JMEPEG (2018) 27:3699–3708
https://doi.org/10.1007/s11665-018-3426-3

1059-9495/$19.00

Tribological Behavior of a Cr_2O_3 Ceramic Coating/Steel Couple Under Dry Sliding and Heavy Loading Conditions

C. Soffritti, M. Merlin, R. Vazquez, and G.L. Garagnani

(Submitted November 11, 2017; in revised form February 28, 2018; published online May 25, 2018)

This work evaluates the effects of heavy loadings on a Cr_2O_3 ceramic coating/steel couple under dry sliding and in conditions similar to those occurring in heavy-duty diesel engines. Two types of wear tests were performed by a standard pin-on-disc tribometer under high constant and variable loads. Before wear tests, microstructure and mechanical properties of coating and steel were determined by optical emission spectrometry, optical microscopy, roughness, microhardness and x-ray diffractometry (XRD). The friction coefficient was directly calculated by the tribometer. The wear rate of Cr_2O_3 ceramic coating was evaluated by the wear volume and that of pins by weighing them before and after tests. The wear tracks on pins and coating surfaces were analyzed by XRD and by scanning electron microscopy with energy-dispersive spectroscopy. For all loads except the lowest constant one, the results indicated high friction and wear involving material removal from the coating surface, through a severe-oxidational wear associated with extensive cracking of the surface of the coating, softening of the carburizing steel and removal of the carburized layer of pins. The wear mechanism was mild-oxidational under the lowest constant load, which was therefore suggested as the limit for acceptable performance of the sliding couple under study.

Keywords carburizing steel, diesel engines, heavy loadings, plasma-sprayed coatings, wear

1. Introduction

Over the last decade, much effort has been made to improve the performance of diesel engines in terms of fuel efficiency and limiting key pollutants. Some of these improvements include the possibility of operating on engine subsystems such as the engine block with pistons and cylinders, the transmission, the fuel system, the valve train and the exhaust system (Ref 1). Concerning wear resistance of mechanical components, when common thermo-mechanical processes and heat treatments are inadequate, thermal-sprayed ceramic coatings on steel may be considered. These coatings are able to withstand high temperatures, are resistant to many corrosive environments and exhibit high hardness and chemical stability. Some types of ceramics have already been applied in engineering as tribological components, for example in cylinder head fire decks, piston crowns, exhaust valve faces and braking devices (Ref 2). Among thermal-sprayed ceramic coatings, plasma-sprayed Cr_2O_3 coatings are an excellent choice because of their low friction coefficients: they can be conveniently deposited on piston ring and cylinder liners in the automotive industries. Under dry sliding conditions, plasma-sprayed Cr_2O_3 coatings are known to form a tribofilm composed of a compacted and plastically deformed wear debris, lowering friction coefficients (Ref 3). Moreover, the low roughness of as-sprayed surface reduces the number of mechanical treatments required after coating for many applications (Ref 4, 5).

Several studies deal with the sliding wear resistance of ceramics against steel (Ref 6-9), and concerning plasma-sprayed Cr_2O_3 coatings, a wear increases with increased load and sliding speed has been observed (Ref 10). The effects of high normal loads and relative humidity on tribological behavior of a sliding couple plasma-sprayed Cr_2O_3 coating/steel have been examined: the results showed that the wear rates of ceramic coating decreased with load in dry and wet conditions, while those of steel were independent of load in dry conditions (Ref 11).

In common operating conditions, most components under mechanical loading undergo dynamic rather than static stresses. Recently, the effects of variable loads on wear resistance of carbon steel in unlubricated condition have been extensively investigated (Ref 12, 13) and a "quasi-mild wear mode" has been proposed, resulting from formation of a work-hardened, severely oxidized surface under heavier loads. The appearance of the quasi-mild wear was apparently affected by several factors such as the sliding distance at low loads before a load increase, the morphology of wear debris, the flattening and degree of oxidation of the worn surfaces (Ref 14, 15).

The effects of heavy loadings have been previously investigated in medium duty diesel engines for Cr_2O_3-Mo composite coatings in dry sliding conditions (Ref 16), using bench tests. More recently, the same coatings have been tested in similar conditions under heavy loadings using a pin-on-disc tribometer (Ref 17). Our study investigates the tribological effects of heavy loadings on plasma-sprayed Cr_2O_3 ceramic coating in dry sliding contact with carburizing steel, in conditions similar to those occurring in heavy-duty diesel engines. Two types of wear tests were conducted, respectively, under high constant and variable loads using a standard pin-on-disc tribometer.

2. Experimental Details

A plasma-sprayed Cr_2O_3 ceramic coating, 150-µm thick (feedstock powder: Amperit®, − 45 + 22.5 µm, fused and

C. Soffritti, M. Merlin, R. Vazquez, and **G. L. Garagnani**, Department of Engineering, University of Ferrara, Via Saragat 1, 44122 Ferrara, Italy. Contact e-mail: chiara.soffritti@unife.it.

crushed), laid on a Ni-20%Cr bond coat about 20 μm thick (feedstock powder: Metco 43CNS, − 106 + 45 μm) to improve the ceramic material adhesion, was deposited onto circular steel discs (80 mm in diameter and 6 mm in thickness). The spray parameters were confidential. A SPECTROLAB OES analyzer (SPECTRO Analytical Instruments GmbH, Kleve, Germany) was used to determine the chemical composition of the steel discs and pins used for wear tests. The compositions of powders were directly provided by the manufacturer. Details of the chemical composition of the feedstock powders, steel discs and pins are shown in Table 1.

The coating microstructure was investigated by x-ray diffractometry (XRD) with a Philips X'PERT PW3050 diffractometer (Philips, Amsterdam, Netherlands), using Cu K-alpha radiation (λ = 1.54 Å), with an intensity scanner versus diffraction angle between 15° and 120° (0.06° step size, 2 s/step scanner velocity and 1.5 grid), a 40 kV voltage and a 30 mA filament current. Properly polished cross-sections were also examined by a Zeiss EVO MA 15 (Zeiss, Oberkochen, Germany) scanning electron microscope equipped with an Oxford X-Max 50 (Oxford Instruments, Abingdon-on-Thames, UK) microprobe for energy-dispersive spectroscopy (SEM/EDS) and a Leica MEF4 M (Leica, Wetzlar, Germany) optical microscope. The SEM micrographs were recorded in secondary electron imaging (SEI-SEM) and back-scattered electron (BSE-SEM) mode. The optical micrographs were processed by an image analysis software to evaluate coating porosity. Roughness parameters (R_a and R_z) were calculated by a portable Handysurf E35_A ZEISS-TSK rugosimeter (Zeiss). Before each measurement, all coating surfaces were cleaned in an ultrasonic bath. Microhardness (300 g_f load and 15 s loading time) and fracture toughness (1000 g_f load) were measured on polished cross-sections of the coating by a Future-Tech FM-110 Vickers microindenter (Future-Tech Corp., Kawasaki, Japan). A mean of 15 indentations were carried out for each microhardness and toughness measurement. Fracture toughness was evaluated by measuring the length of indentation diagonals and cracks through optical micrographs, employing the Evans–Wilshaw equation:

$$K_{IC} = 0.079\left(\frac{P}{a^{3/2}}\right)\log\left(4.5\frac{a}{c}\right) \quad \text{(Eq 1)}$$

where a is the half-length of indentation diagonal (μm), c is the crack length (μm) and P is the load (mN). This formula was developed for "half-penny-shaped" cracks, but it is considered valid also for Palmqvist cracks when the ratio between the crack and the half-length of diagonal indentation is between 0.6 and 4.5 (Ref 18, 19).

Pin-on-disc dry sliding tests were performed with a Multispecimen Tester tribometer (Ducom Instruments, Bengaluru, India) in accordance with ASTM G99-05, using cylindrical steel pins of 6 mm in diameter and 22 mm in height as a counterpart material. All unworn surfaces of original pins were carburized up to about 500 μm in depth. This value represents the effective thickness, i.e., the thickness of the material layer with hardness equal or greater than 550 $kg_f\,mm^{-2}$ (Ref 20). The pins were then oil-quenched from 870 ± 5 °C and tempered at 180 ± 5 °C. The Vickers microhardness (500 g_f load and 15 s loading time) was determined on cleaned cross-sections of the pins by the Future-Tech FM-110 microindenter (Future-Tech Corp.). The measurements were taken at a distance of about 100 μm from the sliding interface, up to about 5 mm in depth. The wear tests were carried out under two different conditions of normal load: (1) under constant load of 250, 450 and 650 N, at a sliding speed of 1 m/s and sliding distance of 7500 m; (2) under variable load in a range between 250 and 650 N, with an increase of 100 N every 40 min (corresponding to a sliding distance of 2400 m), at a sliding speed of 1 m/s and sliding distance of 12,000 m. All tests were performed at room temperature, in dry conditions. For each condition of applied load, five wear tests were conducted. The total wear of pins and discs was measured by a Gefran PY-2-F-010-S01 M linear voltage resistance transducer (LVRT) (Gefran, Brescia, Italy) (accuracy: 1 μm) and quantified with a potentiometric wear measuring device. The friction coefficient was directly calculated by the tribometer. The wear rate of discs was evaluated by measuring the cross-section area of the wear track with a Talysurf CCI-Lite non-contact 3D profilometer (Taylor-Hobson, Leicester, UK). Each area value, obtained as an average of four measurements of cross-section areas along the track, was used to calculate the wear volume. The wear rate of pins was evaluated by weighing them before and after tests. Weight loss was converted into volume loss by dividing it by the material density. The wear depth of pins was calculated by measuring the decrease in length by calipers before and after tests. In order to clarify the wear mechanisms, the worn surfaces of the coating were investigated by XRD with the Philips X'PERT PW3050 diffractometer (Philips). The wear tracks on pins and coating surfaces were then observed by SEM/EDS with the Zeiss EVO MA 15 scanning electron microscope (Zeiss) equipped with the Oxford X-Max 50 microprobe (Oxford Instruments) for semi-quantitative EDS analyses. Finally, the worn cross-sections of pins were characterized by optical microscope analyses with the Leica MEF4 M (Leica) and Vickers microhardness measurements at 500 g_f load and 15 s loading time by the Future-Tech FM-110 microindenter (Future-Tech Corp.). As performed on original pins, the Vickers microhardness measurements were taken at a distance of about 100 μm from the sliding interface, up to about 5 mm in depth.

Table 1 Chemical composition of feedstock powders, steel discs and pins used for wear tests

	Chemical composition, wt.%
Ceramic coating	0.06 SiO_2; 0.03 Fe_2O_3; < 0.02 TiO_2; balance Cr_2O_3
Bond coat	19.07 Cr; 1.10 Si; 0.40 Fe; 0.02 C; balance Ni
Disc	0.22 C; 0.88 Mn; 0.87 Ni; 0.84 Cr; 0.30 Si; 0.20 Cu; 0.06 Mo; 0.03 S; 0.02 V; 0.02 P; balance Fe
Pin	0.23 C; 0.86 Mn; 0.95 Ni; 0.91 Cr; 0.26 Si; 0.10 Cu; 0.06 Mo; 0.02 S; 0.02 V; 0.01 P; balance Fe

3. Results

3.1 Microstructure and Mechanical Properties

The BSE-SEM micrographs of the microstructure observed on the cross-section of Cr_2O_3 coating before wear tests are shown in Fig. 1(a) and (b). The Cr_2O_3 coating exhibited the typical lamellar microstructure of a plasma-sprayed ceramic coating, characterized by a prevalence of inter-lamellar cracks (at splat boundaries), uniformly distributed pores and very few unmolted particles (Fig. 1a). The inter-lamellar cracks, caused by thermal residual stresses, were mostly responsible for the low inter-splat cohesion of the coating. The Ni-20%Cr bond coat was markedly irregular, with pores and sandblast residues visible at the bond coat/steel interface, favoring the adhesion of the coating to the substrate (Fig. 1b). The porosity was about 11%, as determined by image analysis, due to splat stacking faults and gas entrapment. The XRD diffractograms recorded on the surface of Cr_2O_3 coating before wear tests revealed that the coating was all in the eskolaite phase (hexagonal Cr_2O_3) (Fig. 2). The mean value of Vickers microhardness measured on the coating cross-sections was 11.88 ± 0.45 GPa, whereas those of the roughness parameters were 0.15 ± 0.02 μm (R_a) and 1.78 ± 0.19 μm (R_z). The mean fracture toughness of the Cr_2O_3 coating calculated by Eq 1 was 7.16 ± 0.88 MPa $m^{1/2}$.

An optical micrograph of the cross-section of pins before wear tests is shown in Fig. 3, together with the Vickers microhardness profile resulting from the carburizing treatment. The microstructure of the carburized layer was martensitic with low carbide content, and that of the non-carburized material was lower bainitic. The Vickers microhardness was maximum at the surface and then decreased toward the inside, finally reaching the typical value of non-carburized steel. The Vickers microhardness profile also confirmed an effective thickness of about 500 μm for the carburizing treatment.

3.2 Friction and Wear Curves

The friction coefficient and the total wear variations calculated during the tests under constant load (250, 450 and 650 N) and under variable load (from 250 to 650 N) are shown in Fig. 4.

Under a constant 250 N load (Fig. 4a), the friction coefficient raised rapidly during the first few minutes and reached the quasi-steady state (μ ≅ 0.10) at only 150 m. The values gradually increased up to about 0.20, from a sliding distance of about 2000 m onward. Under constant loads of 450 and 650 N (Fig. 4b and c), the friction coefficient curves followed a similar pattern. At the beginning of each test, the coefficients were low (between 0.10 and 0.20) and then rapidly increased: after about 1000 m for 450 N and 2500 m for 650 N, the values reached a quasi-steady state (between 0.30 and 0.40), maintained until the end of tests. Under variable load (Fig. 4d), the friction coefficient variations were similar to those observed under constant load of 450 and 650 N. Severe running-in wear took place until 650 m, after which a quasi-steady state (μ ≅ 0.35) was reached. Nevertheless, small μ variations could be observed at sliding distances of about 2400, 5000, 7500 and 10,000 m, corresponding to the transitions 250/350, 350/450, 450/550 and 550/650 N in the applied load. When the mean friction coefficients were calculated over the five tests, those under the higher constant loads and the variable load resulted similar (between 0.34 and 0.38), but that under the constant load of 250 N was about 36% lower (μ = 0.23).

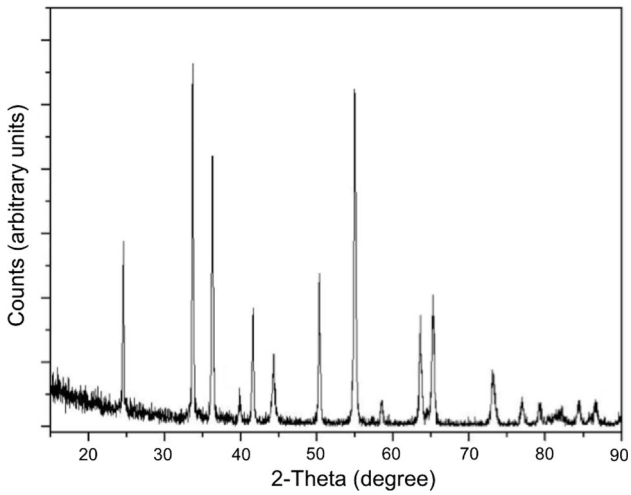

Fig. 2 XRD diffractogram recorded on the surface of Cr_2O_3 coating before wear tests. The position of peaks indicates that the Cr_2O_3 coating is all in the eskolaite phase

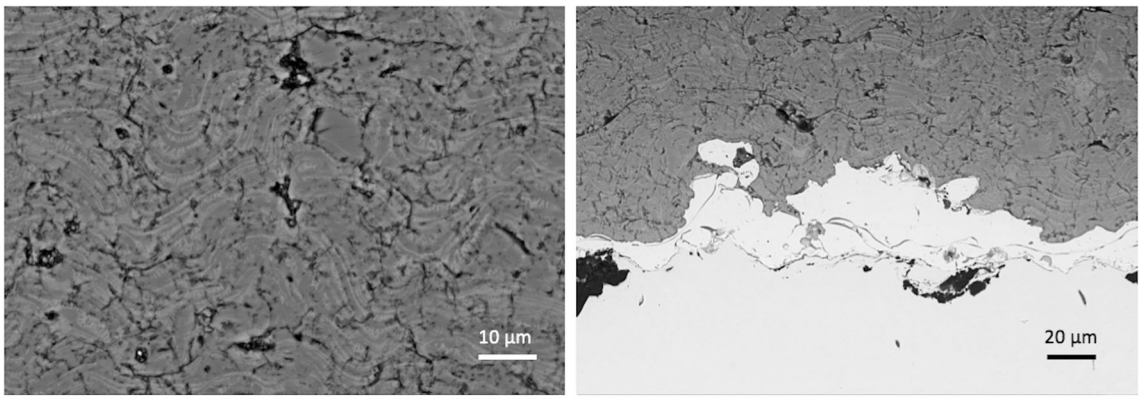

Fig. 1 BSE-SEM micrographs of the microstructure of Cr_2O_3 coating, observed in the cross-section before wear tests: details of the coating (a) and of the Ni-20%Cr bond coat (b)

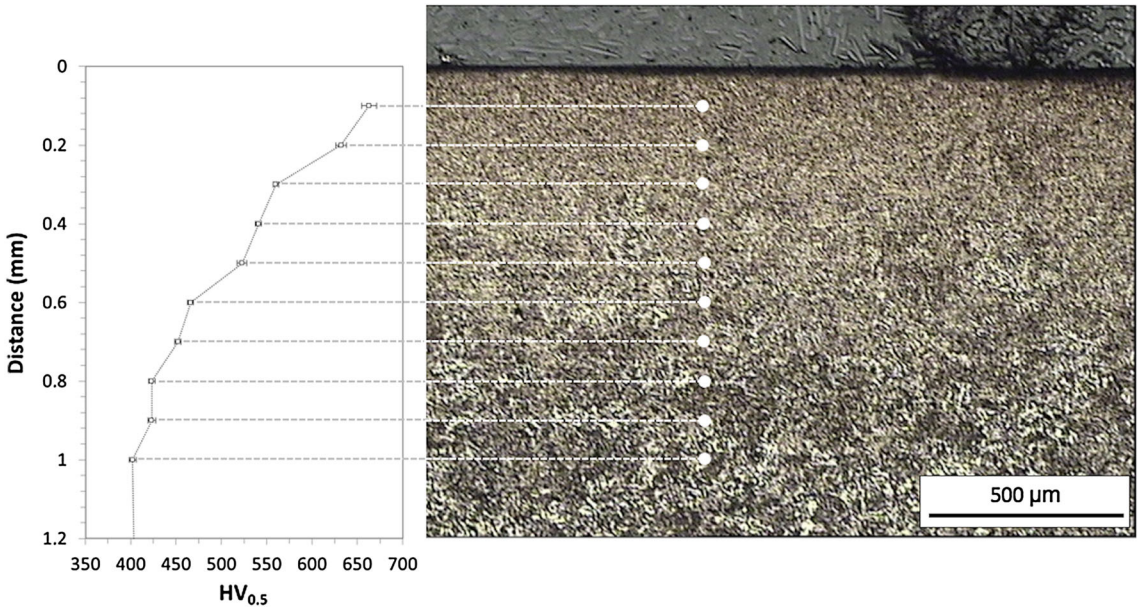

Fig. 3 Optical micrograph of the microstructure of pins in cross-section before wear tests (on the right) and the Vickers microhardness profile resulting from the carburizing treatment (on the left), measured from 0.1 mm from the sliding interface up to 1 mm in depth

Concerning the total wear variation, under a constant 250 N load the values were all negative until the end of tests (Fig. 4a). Under the constant loads of 450 and 650 N (Fig. 4b and c), the total wear curves followed a similar pattern. For 450 N, the total wear was negative up to a sliding distance of about 3500 m, and then it progressively increased, reaching a final positive value of about 0.29 mm (Fig. 4b). For 650 N, the total wear was negative up to about 5000 m and increased, reaching a final positive value of about 0.45 mm (Fig. 4c). Under variable load, the total wear variation was negative until a sliding distance of about 1500 m, then slowly increased, reaching a final positive value of about 0.65 mm (Fig. 4d). At least two slope changes could be observed, the first one at a sliding distance of about 4000 m and under 350 N load, and the second one at about 10,000 m, corresponding to the 550/650 N transition in the applied load.

An example of a 3D surface profilometry of the wear track on Cr_2O_3 coating under the constant 650 N load is shown in Fig. 5 together with the mean wear rates of Cr_2O_3 coating and of pins in all conditions tested. When the higher constant load and the variable loading conditions were applied, the cross-section profiles of the worn disc surfaces were characterized by alternating convex and concave regions (Fig. 5a). The convex regions became smoother and the concave regions were reduced with an increase in constant load and under variable load. In the same conditions, other peaks could be seen at the edges of the wear track. For the constant 250 N load, the wear damage was negligible and the wear track profile generally followed the roughness of Cr_2O_3 coating. When all 3D profilometry data were considered, the depth of the wear tracks increased in the following order: 250 < 450 < 250-650 < 650 N.

Concerning the mean wear rates of Cr_2O_3 coating and of pins (Fig. 5b), the mean wear rates of the coating were approximately 1-3 $\times$ 10^{-6} mm^3 N^{-1} m^{-1} for the constant loads of 450 and 650 N and the variable load, while the mean wear rate under the constant 250 N load was the lowest ($\cong$ 10^{-8} mm^3 N^{-1} m^{-1}). The mean wear rates of pins in all conditions tested ranged from 1 to 6 $\times$ 10^{-6} mm^3 N^{-1} m^{-1}.

The SEI-SEM micrographs of the worn surface of Cr_2O_3 coating after wear tests under variable load are shown in Fig. 6(a), (b), and (c). The morphology of the worn surface of the coating (Fig. 6a) was characterized by two features: material removal with pits and microcracks randomly distributed over the wear track (Fig. 6b) and metallic film deposition (Fig. 6c). In the first case, particles were visible inside pits and, according to the microstructure of Cr_2O_3 coating, microcracks occurred perpendicularly along individual ceramic lamellae and their columnar grain interfaces. Many microcracks could also be seen along the splat boundaries, parallel to the surface. In the second case, the tribofilm appeared to crack more or less perpendicularly to the sliding motion; it was firmly attached to Cr_2O_3 coating, plastically deformed and oriented along the reciprocating pin direction. Comparing the semi-quantitative EDS analyses of the elements in the tribofilm and in other regions, the percentage of iron in the tribofilm was about twice than in the rest of the wear track (Fig. 7). The XRD examinations on the tribofilm confirmed these data, identifying Fe_2O_3 and showing that the crystal structure of Cr_2O_3 coating was unchanged after the tests (Fig. 8).

For the constant loads of 450 and 650 N, the morphology of the worn surfaces of Cr_2O_3 coating was similar to that under variable load and the amount of metal transfer could be compared to the metallic film deposition observed in Fig. 6(a), but the pits were shallow. Under the constant 250 N load, the wear track of the coating appeared smoother and oxidized (Fig. 9a) and microcracks and spalled iron oxides could be observed at higher magnification in some places (Fig. 9b).

The SEI-SEM micrographs of the worn surfaces of pins after wear tests under variable load and the constant 250 N load are shown in Fig. 10. Under variable load and constant loads of 450 and 650 N, a metallic film of iron oxide uniformly covered the worn surfaces: it was very rough and plastically deformed

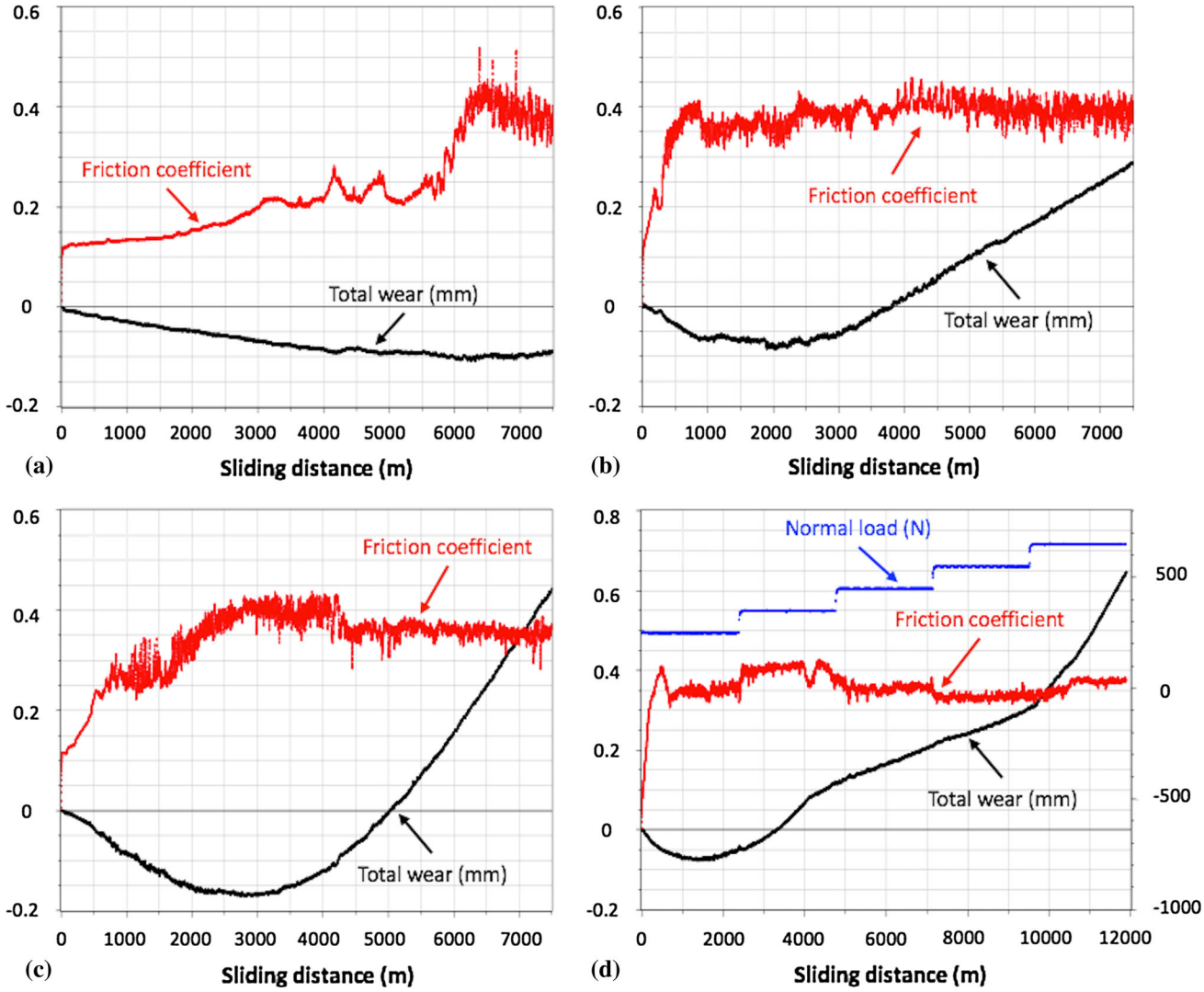

Fig. 4 Friction coefficient and total wear variations under the different conditions of normal load: (a) constant 250 N load; (b) constant 450 N load; (c) constant 650 N load; (d) variable 250-650 N load

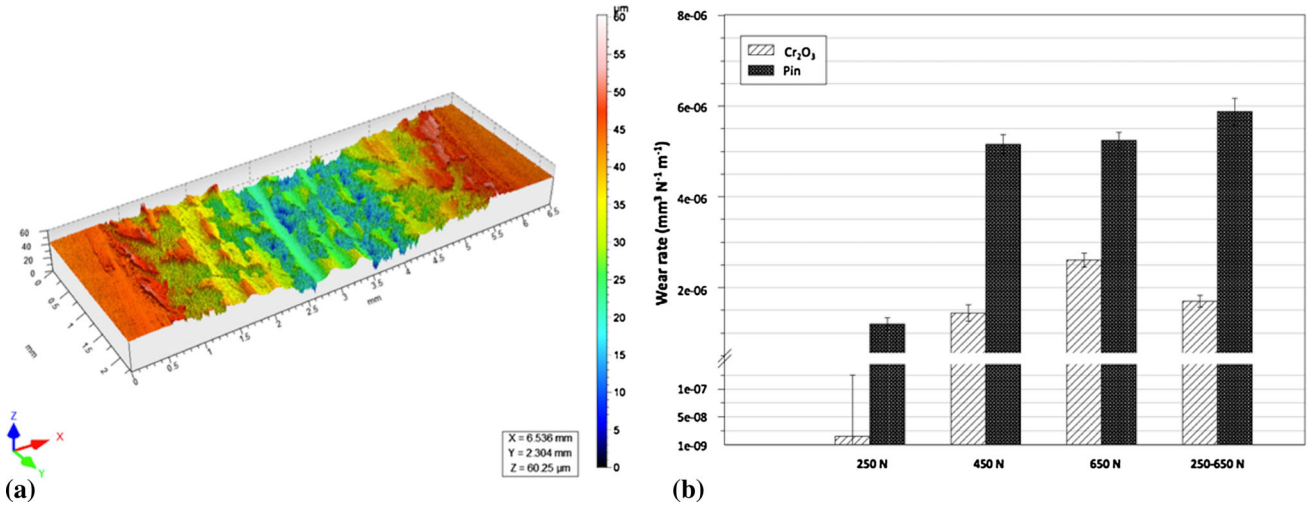

Fig. 5 Example of a 3D surface profilometry of the wear track on Cr_2O_3 coating under the constant 650 N load (a) and mean wear rates of Cr_2O_3 coating and of pins in all conditions tested (b). Error bars represent standard deviation

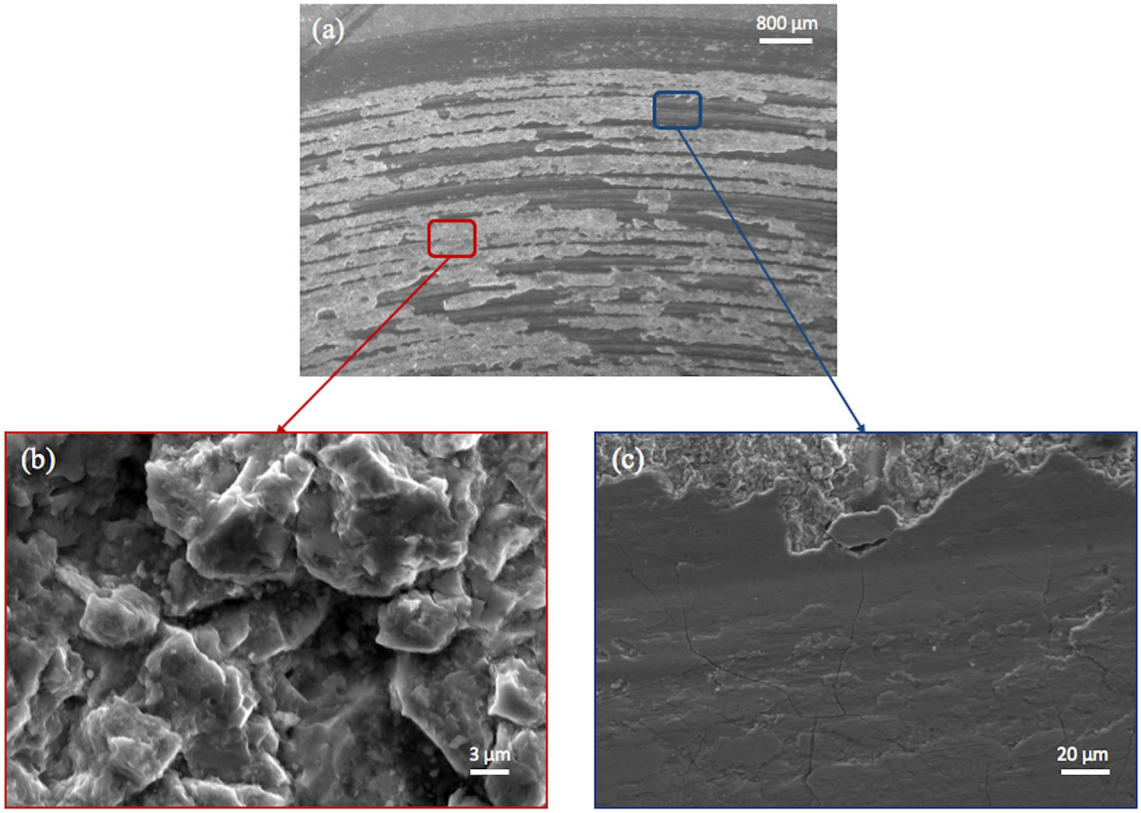

Fig. 6 SEI-SEM micrographs of the worn surface of Cr_2O_3 coating after wear tests under variable load: (a) overview of wear track; (b) details of pits and microcracks, showing particles inside pits; (c) detail of cracked and plastically deformed tribofilm

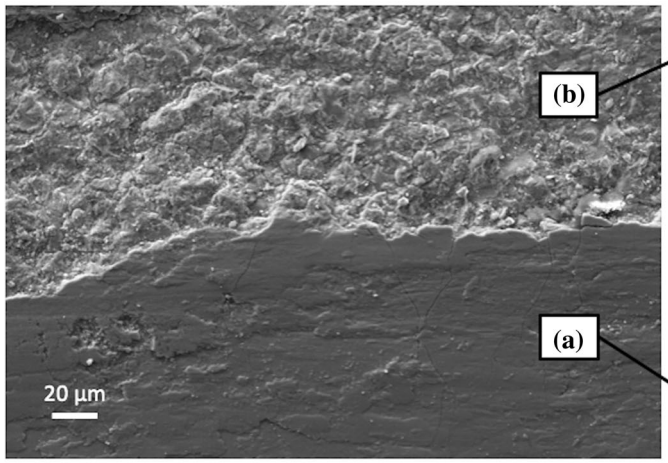

Element	Wt.%
C K	3.58
O K	35.85
Si K	0.10
Cr K	47.30
Fe K	13.17
Totals	100.00

Element	Wt.%
C K	5.92
O K	24.85
Si K	0.09
Cr K	40.07
Fe K	29.07
Totals	100.00

Fig. 7 SEI-SEM micrograph of the wear track on Cr_2O_3 coating after wear test under variable load and semi-quantitative EDS analyses (wt.%) of the tribofilm (a) and of another region of the wear track (b)

with plowing and cutting appearance (Fig. 10a). For the constant 250 N load, the morphology of the worn surfaces of pins was similar, but with a lower amount of metallic oxide (Fig. 10b).

Under variable load and the higher constant loads, optical microscope observations of pins showed that the sliding wear between Cr_2O_3 coating and carburizing steel resulted in a layered microstructure (Fig. 11). In cross-section and beginning from the worn surface, the microstructure was composed of a spalled iron oxide layer about 10 µm thick with a dark gray color, a very fine and unoriented layer, a fine and oriented layer, a plastically deformed layer and the unaffected microstructure. For the constant 250 N load, the layers of the microstructure were smaller (Fig. 12): the spalled iron oxide layer was less than 10 µm thick and between this layer and the fine oriented one a new discontinuous layer could be observed.

Microhardness profiles of the cross-sections of pins before and after wear tests in all conditions are shown in Fig. 13, together with the mean wear depths of pins. For the constant loads of 450 and 650 N and the variable load, the microhardness profiles followed a similar pattern: the microhardness was very low at a distance of about 100 µm from the sliding interface, then progressively increased, reaching a value comparable to that of the original pin. For the constant 250 N load, the microhardness was still very low at a distance of about 100 µm from the sliding interface: from 200 µm inward, the microhardness profile was comparable to that of the original pin and typical of carburized steel.

Concerning the mean wear depths of pins calculated over the five tests, those under the variable load and the constant 650 N load were greater than the effective thickness for the carburizing treatment and equal to 1.10 and 0.91 mm, respectively. The values of mean wear depth of pins therefore decreased with the decrease in constant load values. The mean wear depths at 450 and 250 N, respectively, 0.32 and 0.08 mm, were both lower than the effective thickness for the carburizing treatment.

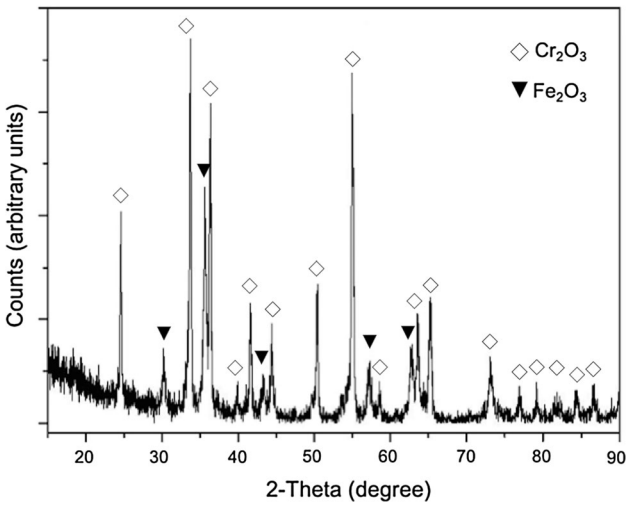

Fig. 8 XRD diffractogram recorded on the surface of Cr_2O_3 coating after wear tests. The peaks of the crystal structure of Cr_2O_3 coating are similar to those of Fig. 2

4. Discussion

Wear tests under heavy constant and variable loading conditions were performed for investigating friction and wear resistance of a plasma-sprayed Cr_2O_3 ceramic coating in dry sliding contact with carburizing steel. The pin-on-disc wear tests show a rise in the friction coefficient positively correlated with the metal transfer from pins onto Cr_2O_3 coating surfaces detected by SEM/EDS. Similarly, negative total wear suggests pin lifting due to the build-up of material under high temperatures at the surface. The SEM/EDS images show a compact tribofilm due to wear particles sufficiently small to penetrate the grooves and later be sintered by high temperatures (Ref 7, 21). As sliding continues, the total wear becomes positive for all loads except the constant 250 N load. This is due to the fragmentation of the tribofilm: its surface layers, partially removed, may produce free moving particles between the sliding surfaces, acting as three-body abrasive (Ref 21). The surface 3D profilometry also suggests that some of these particles could be expelled from the contact interface and accumulated along the edges of the wear track. For plasma-sprayed Cr_2O_3 ceramic coating/steel couple tested in this study, the mean friction coefficients under variable load and constant loads of 450 and 650 N are between 0.34 and 0.38, whereas for the constant 250 N load, the mean friction coefficient is 0.23.

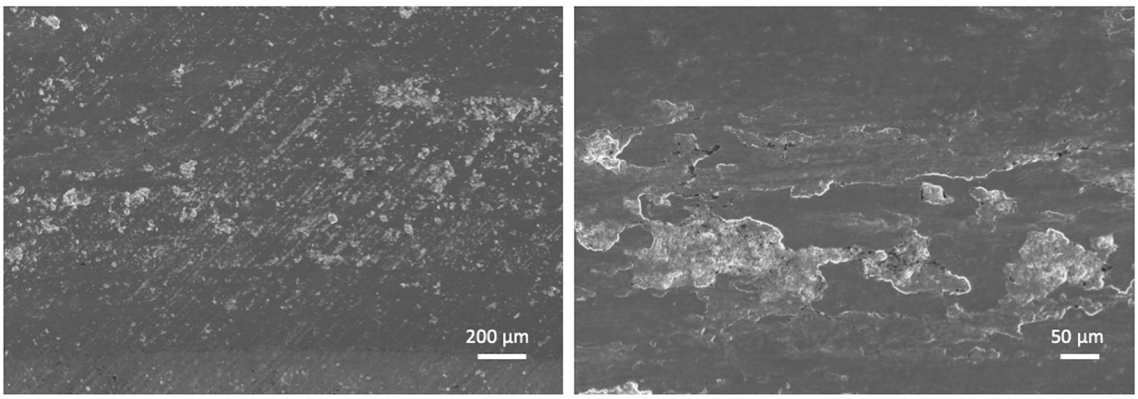

Fig. 9 SEI-SEM micrographs of the worn surface of Cr_2O_3 coating after wear tests under the constant 250 N load: overview of wear track (a) and details of microcracks and spalled iron oxides (b)

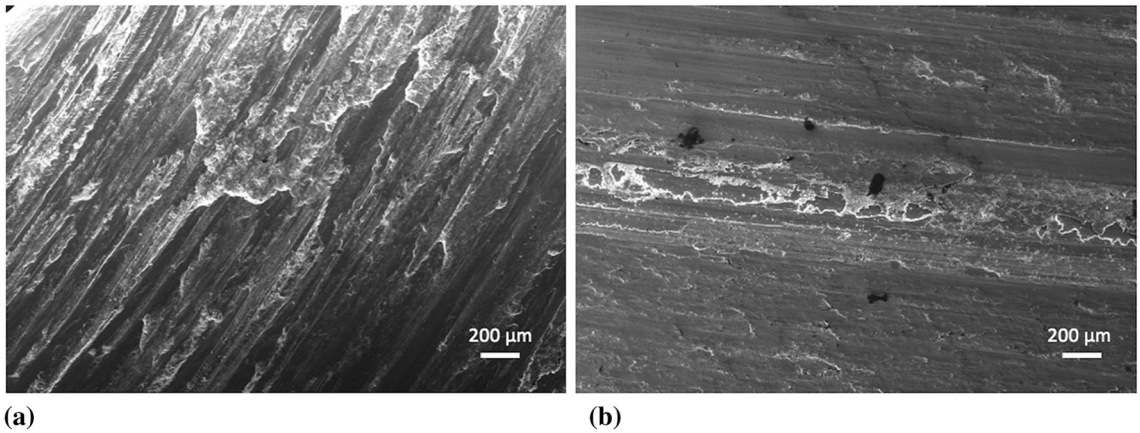

Fig. 10 SEI-SEM micrographs of the worn surfaces of pins after wear tests under variable load (a) and under the constant 250 N load (b)

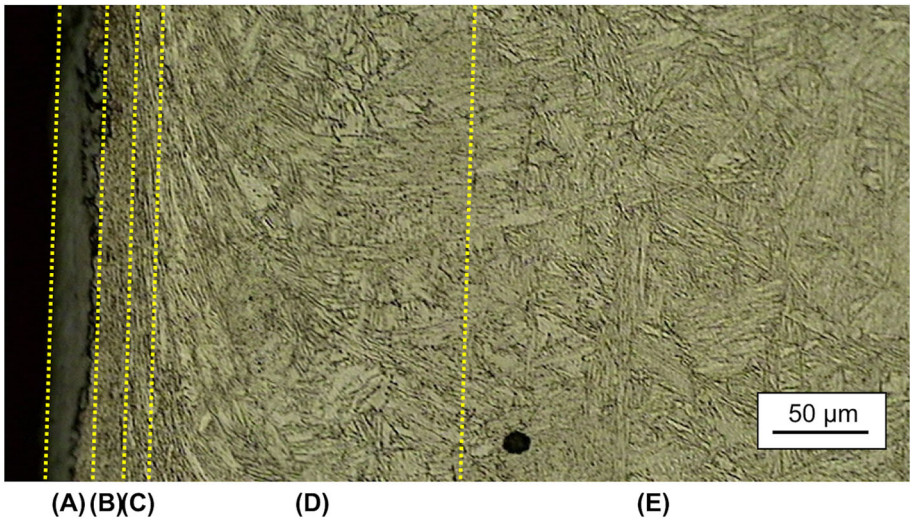

Fig. 11 Optical micrograph of the layered microstructure observed on the cross-section of pins after wear tests under variable load. The yellow dashed lines indicate the boundaries between layers. From left to right: spalled iron oxide layer (A), fine unoriented layer (B), fine oriented layer (C), plastically deformed layer (D), unaffected microstructure (E) (Color figure online)

Fig. 12 Optical micrograph of the layered microstructure observed on the cross-section of pins after wear tests under the constant 250 N load. The yellow arrow indicates the new discontinuous layer between the spalled iron oxide layer and the fine oriented one

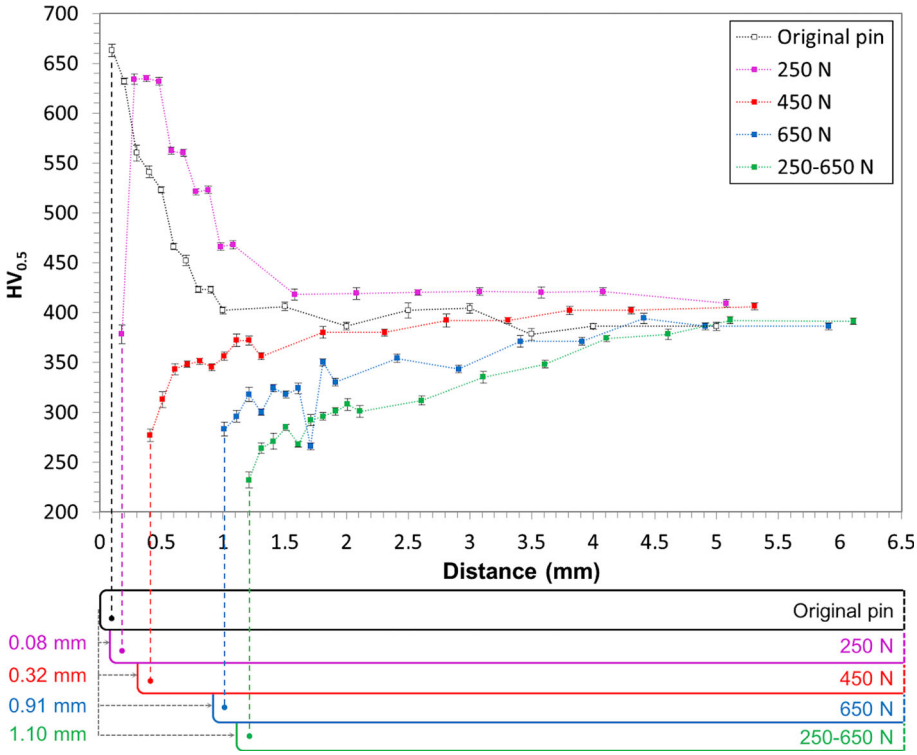

Fig. 13 Microhardness profiles of the cross-sections of pins before and after wear tests in all conditions examined, at different distances (mm) from the sliding interface. Each microhardness value was measured in triplicate. Error bars represent standard error. The lower part of the figure reports the mean wear depths of pins (mm) in the same conditions

The recorded values are comparable to previously reported μ values for plasma-sprayed Cr_2O_3 ceramic coating/steel couples under dry sliding conditions (Ref 3, 8-11).

The mean wear rates of Cr_2O_3 coating under variable load and constant loads of 450 and 650 N are much higher ($\cong 10^{-6}$ mm^3 N^{-1} m^{-1}) than that under the constant 250 N load ($\cong 10^{-8}$ mm^3 N^{-1} m^{-1}). Comparing our mean wear rates of Cr_2O_3 coating with previous research on wear of sintered ceramics (Ref 22, 23), the present Cr_2O_3 coating is under a severe wear regime for all loads except at the constant 250 N load where the wear regime is between mild and severe. In all conditions tested, the mean wear rates of pins are about 10^{-6} mm^3 N^{-1} m^{-1}. Studies on wear resistance of high carbon steels under dry sliding state that when the mean wear rate is higher than 1×10^{-8} mm^3 N^{-1} m^{-1}, the wear should be considered severe (Ref 24-26). The severe wear detected in our study is also supported by SEM/EDS images.

The morphology of the wear track on Cr_2O_3 coating indicates that during dry sliding, wear debris is entrapped in the contact interface and undergoes continued fracture and deformation, producing particles detected by SEM/EDS. The tribofilm detected by the same analysis suggests an oxidational wear mechanism. Previous research showed that, under a mild-oxidational wear regime, oxidation is caused by frictional heating (Ref 21). In this case, if the tribofilm is firmly attached to the ceramic coating, it may thicken and provide protection against further wear damage until it reaches a critical thickness (about 10 μm for steel, as confirmed by our optical microscope observations), then it can spall off as wear debris (Ref 7, 21). The SEM/EDS and optical microscope images indicate that a transition to severe-oxidational wear regime occurs for all loads except the constant 250 N load. This transition associated with extended oxidation is supported by the fact that the tribofilm is thicker and more plastic at these loads (Ref 8, 13, 21, 26-28). In our study, the oxide layer is identified as Fe_2O_3 by EDS and XRD examinations. It is known that, for plasma-sprayed Cr_2O_3 ceramic coating in dry sliding contact with steel, Fe_2O_3 is formed when the temperature at the contact surface rises over 200 °C and remains stable when the temperature lowers until 25 °C (Ref 10, 11).

On the cross-sections of pins, the layered microstructure detected by optical microscopy suggests that severe-oxidational wear involves a series of processes, such as plastic deformation and shear fracture of surface layers. These observations show that the thickness of the plastically deformed layer increases with increasing load and under variable load, due to the low thermal conductivity of martensitic + carbide microstructure (Ref 24, 25). Moreover, a new layer is observed between the iron oxide layer and the fine oriented one for the constant 250 N load. Previous research showed that during dry sliding, the three-dimensional compressive stresses on the layers nearest to the contact surface may lower the martensite start temperature, transforming it in austenite which could be partially retained after friction (Ref 26, 28), as observed in this study in Fig. 12. No austenite was found in our study under variable load and the higher constant loads. It was previously shown that at high loads the amount of austenite sharply decreases due to softening of the material in the layers nearest to the contact surface (Ref 26). The microhardness profiles of the cross-sections of pins obtained after the wear tests under the constant loads of 250 and 450 N suggest a softening of the martensitic + carbide microstructure associated with a partial removal of the carburized layer. Under the constant 650 N and variable load, the microhardness profiles indicate the softening

of the lower bainitic microstructure and the total removal of the carburized layer. Wear resistance is known to be negatively related to the softening behavior of worn surface layers (Ref 24-26): in our wear tests, the softening of the material under variable load and higher constant loads is accordingly related to a worsening of wear resistance.

5. Conclusions

The effects of heavy loadings on a plasma-sprayed Cr_2O_3 ceramic coating/steel couple were evaluated under dry sliding and in conditions similar to those occurring in heavy-duty diesel engines. The pin-on-disc wear tests were conducted under high constant and variable loads. The results showed high friction and wear involving both material removal from the coating surface and oxidational wear. The dry sliding of carburizing steel over Cr_2O_3 ceramic coating produced a Fe_2O_3 metallic film transferred on the ceramic surface. Under the constant 250 N load, the thickness of the metallic film was under the critical value of 10 μm, thus classifiable as mild-oxidational wear; however, microcracks and spalled iron oxides were observed over the wear track. Under the constant loads of 450 and 650 N and the variable load, the thickness of the metallic film reached the critical value and a transition from mild- to severe-oxidational wear occurred. This transition was associated with extensive cracking of the surface of plasma-sprayed Cr_2O_3 ceramic coating, softening of the carburizing steel and removal of the carburized layer of pins. Based on our results, it can be concluded that the usefulness of the plasma-sprayed Cr_2O_3 ceramic coating/steel couple under dry sliding and in heavy-duty diesel engines may be limited to applied loads lower than 250 N.

Acknowledgments

The authors would like to thank Zocca Officine Meccaniche (Funo, Bologna, Italy) for the thermally sprayed coating manufacturing, and Engineer Marco Vitali for his contribution to the experimental activity. The authors thank Dr. Milvia Chicca for help in revising the manuscript. This work was supported by the Department of Engineering, University of Ferrara (Ferrara, Italy), Grant No. 2238/2010.

References

1. H.A. Bolton and J.M. Larson, *Valvetrain System Design and Materials*, ASM International, Materials Park, Ohio, 2002
2. S. Asanabe, Applications of Ceramics for Tribological Components, *Tribol. Int.*, 1987, **20**, p 355–364
3. G. Bolelli, V. Cannillo, L. Lusvarghi, and T. Manfredini, Wear Behaviour of Thermally Sprayed Ceramic Oxide Coatings, *Wear*, 2006, **261**, p 1298–1315
4. F. Rastegar and A.E. Craft, Piston Ring Coatings For High Horsepower Diesel Engines, *Surf. Coat. Technol.*, 1993, **61**, p 36–42
5. P. Ernst and G. Barbezat, Thermal Spray Applications In Powertrain Contribute to the Saving of Energy and Material Resources, *Surf. Coat. Technol.*, 2008, **202**, p 4428–4431
6. V. Aronov and T. Mesyef, Wear in Ceramic/Ceramic and Ceramic/Metal Reciprocating Sliding Contact Part 1, *J. Tribol.*, 1986, **108**, p 16–21
7. G.W. Stachowiak, G.B. Stachowiak, and A.W. Batchelor, Metallic Film Transfer During Metal–Ceramic Unlubricated Sliding, *Wear*, 1989, **132**, p 361–381
8. B. Wang, Z.R. Shui, and A.V. Levy, Sliding Wear of Thermally Sprayed Chromia Coatings, *Wear*, 1990, **138**, p 93–110
9. H. Cetinel, E. Celik, and M.I. Kusoglu, Tribological Behaviour of Cr_2O_3 Coatings as Bearing Materials, *J. Mater. Process. Technol.*, 2008, **196**, p 259–265
10. J.E. Fernández, Y. Wang, R. Tucho, M.A. Martin-Luengo, R. Gancedo, and A. Rincón, Friction and Wear Behaviour of Plasma-Sprayed Cr_2O_3 Coatings Against Steel in a Wide Range of Sliding Velocities and Normal Loads, *Tribol. Int.*, 1996, **29**, p 333–343
11. M. Merlin, C. Soffritti, and R. Vazquez, Effect of Relative Humidity and Applied Loads on the Tribological Behaviour of a Steel/Cr_2O_3-Ceramic Coupling, *Wear*, 2013, **303**, p 371–380
12. H. Goto and Y. Amamoto, Effect of Varying Load on Wear Resistance of Carbon Steel Under Unlubricated Conditions, *Wear*, 2003, **254**, p 1256–1266
13. H. Goto, Y. Amamoto, and C.V. Suciu, Investigations on the Mechanism of Quasi-Mild Wear for Carbon Steel in Dry Sliding Contact Under Variable Loading, and Endurance of the Worn Surfaces, *Wear*, 2009, **267**, p 505–514
14. H. Goto and Y. Amamoto, Effects of a Stepwise Change in Load on the Subsequent Friction and Wear Characteristics of Carbon Steel Under Dry Sliding, *Wear*, 2007, **263**, p 579–585
15. H. Goto and Y. Amamoto, Improvement of Wear Resistance for Carbon Steel Under Unlubricated Sliding and Variable Conditions, *Wear*, 2011, **270**, p 725–736
16. H.-S. Ahn, I.-W. Lyo, and D.-S. Lim, Influence of Molybdenum Composition in Chromium Oxide-Based Coatings on Their Tribological Behaviour, *Surf. Coat. Technol.*, 2000, **133–134**, p 351–361
17. E. Celik, C. Tekmen, I. Ozdemir, H. Cetinel, Y. Karakas, and S.C. Okumus, Effects on Performance of Cr_2O_3 Layers Produced on Mo/Cast-Iron Materials, *Surf. Coat. Technol.*, 2003, **174–175**, p 1074–1081
18. C.B. Ponton and R.D. Rawlings, Vickers Indentation Fracture Toughness Test—Part 1: Review of Literature and Formulation of Standardised Indentation Toughness Equations, *Mater. Sci. Technol. Ser.*, 1989, **5**, p 865–872
19. C.B. Ponton and R.D. Rawlings, Vickers Indentation Fracture Toughness Test—Part 2: Application and Critical Evaluation of Standardised Indentation Toughness Equations, *Mater. Sci. Technol. Ser.*, 1989, **5**, p 961–976
20. G. Straffelini, *Friction and Wear—Methodologies for Design and Control*, Springer, Cham, 2015
21. F.H. Stott, The Role of Oxidation in the Wear of Alloys, *Tribol. Int.*, 1998, **31**, p 61–71
22. S.M. Hsu and M. Shen, Wear Prediction of Ceramics, *Wear*, 2004, **256**, p 867–878
23. K. Kato and K. Adachi, Wear of Advanced Ceramics, *Wear*, 2002, **253**, p 1097–1104
24. Y. Wang, T. Lei, and J. Liu, Tribo-Metallographic Behaviour of High Carbon Steels in Dry Sliding—I. Wear Mechanisms and Their Transition, *Wear*, 1999, **231**, p 1–11
25. Y. Wang, T. Lei, and J. Liu, Tribo-Metallographic Behaviour of High Carbon Steels in Dry Sliding—II. Microstructure and Wear, *Wear*, 1999, **231**, p 12–19
26. Y. Wang, T. Lei, and J. Liu, Tribo-Metallographic Behaviour of High Carbon Steels in Dry Sliding—III. Dynamic Microstructural Changes and Wear, *Wear*, 1999, **231**, p 20–37
27. H.-S. Ahn and O.-K. Kwon, Tribological Behaviour of Plasma-Sprayed Chromium Oxide Coating, *Wear*, 1999, **225–229**, p 814–824
28. Z.Y. Xu, *Martensitic Transformation and Martensite*, Academic Press, Beijing, 1980